Int. J. Solids Structures Vol. 23, No. 7, pp. 1053–1061, 1987
Printed in Great Britain.

0020-7683/87 $3.00 + .00

DYNAMIC INSTABILITY OF SHEAR DEFORMABLE ANTISYMMETRIC ANGLE-PLY PLATES†

CHARLES W. BERT
School of Aerospace, Mechanical and Nuclear Engineering, University of Oklahoma, Norman, OK 73019, U.S.A.

and

VICTOR BIRMAN
School of Naval Architecture and Marine Engineering, University of New Orleans, New Orleans, LA 70148, U.S.A.

(*Received* 10 *February* 1986; *in revised form* 3 *September* 1986)

Abstract—The effect of shear deformation on dynamic instability of simply supported antisymmetric angle-ply rectangular plates is considered. The boundaries of the principal instability region are conveniently represented in the plane "non-dimensional excitation frequency squared–non-dimensional load amplitude". The effects of the magnitude of the shear correction coefficients, number of layers, plate aspect ratio, and thickness-to-edge length ratio are illustrated in numerical examples.

1. INTRODUCTION

The intensive use of fiber-reinforced composites has resulted in very detailed studies of the static and dynamic behavior of laminated anisotropic plates. The lower transverse shear moduli of such plates makes them much more sensitive to the effect of shear deformation than isotropic plates of the same geometry. Different theories incorporating shear deformation effects were reviewed by Bert[1, 2].

In particular, the theory proposed by Yang *et al.*[3] has been intensively used for solution of both static and dynamic problems. Whitney and Pagano used this theory to study cylindrical bending under transverse load and flexural vibration frequencies of symmetric and unsymmetric laminates[4]. The problems of buckling and free vibrations of shear deformable unsymmetric laminates was discussed by Noor[5] and by Bert and Chen[6].

Notably, Srinivas and Rao[7] as well as Sun and Whitney[8] showed that the theory of Yang–Norris–Stavsky gives satisfactory results for predicting the first flexural modes of vibrations if the transverse shear rigidities of the constituent layers are similar. The effect of unsymmetric lamination on dynamic stability of rectangular plates was considered by Birman[9] who neglected transverse shear deformation and rotary inertia.

In this paper the effect of shear deformation on dynamic stability of antisymmetric angle-ply laminated rectangular plates is studied. The plate is hinged on all edges and the tangential stresses and in-plane displacements in the direction perpendicular to each edge are zero.

2. ANALYSIS

Consider a rectangular antisymmetric angle-ply laminated plate consisting of an even number of identical orthotropic layers oriented alternately at angles $\pm\theta$. The plate is subject to uniformly distributed, parametric, time-dependent loads of intensity $N_1(t)$ and $N_2(t)$ as shown in Fig. 1. The equations of motion of such a plate are[6]

† Presented at the 10th U.S. National Congress of Applied Mechanics, University of Texas, Austin, TX 78712, June 1986.

$$
\begin{aligned}
N_{1,x}+N_{6,y} &= C\rho h u_{,tt} \\
N_{6,x}+N_{2,y} &= C\rho h v_{,tt} \\
Q_{x,x}+Q_{y,y}-N_1(t)w_{,xx}-N_2(t)w_{,yy} &= \rho h w_{,tt} \\
M_{1,x}+M_{6,y}-Q_x &= \frac{\rho h^3}{12}\psi_{x,tt} \\
M_{6,x}+M_{2,y}-Q_y &= \frac{\rho h^3}{12}\psi_{y,tt}
\end{aligned} \tag{1}
$$

where u, v, w are displacements along the x-, y-, z-axes, respectively, ψ_x and ψ_y are the bending slopes in the x–z and y–z planes, t is time, $(\ldots)_{,i} \equiv \partial(\ldots)/\partial i$, ρ is material density, and C is a coefficient of in-plane inertia. The in-plane stress resultants and stress couples are related to the generalized displacements by the following constitutive relations

$$
\begin{Bmatrix} N_1 \\ N_2 \\ N_6 \\ M_1 \\ M_2 \\ M_6 \end{Bmatrix} =
\begin{bmatrix}
A_{11} & A_{12} & 0 & 0 & 0 & B_{16} \\
A_{12} & A_{22} & 0 & 0 & 0 & B_{26} \\
0 & 0 & A_{66} & B_{16} & B_{26} & 0 \\
0 & 0 & B_{16} & D_{11} & D_{12} & 0 \\
0 & 0 & B_{26} & D_{12} & D_{22} & 0 \\
B_{16} & B_{26} & 0 & 0 & 0 & D_{66}
\end{bmatrix}
\begin{Bmatrix} u_{,x} \\ v_{,y} \\ v_{,x}+u_{,y} \\ \psi_{x,x} \\ \psi_{y,y} \\ \psi_{y,x}+\psi_{x,y} \end{Bmatrix}. \tag{2}
$$

The shear stress resultants are functions of the shear correction coefficients k_4^2, k_5^2

$$
\begin{Bmatrix} Q_y \\ Q_x \end{Bmatrix} =
\begin{bmatrix} k_4^2 A_{44} & 0 \\ 0 & k_5^2 A_{55} \end{bmatrix}
\begin{Bmatrix} w_{,y}+\psi_y \\ w_{,x}+\psi_x \end{Bmatrix}. \tag{3}
$$

The extensional, coupling, and bending stiffnesses are defined as

$$
(A_{ij}, B_{ij}, D_{ij}) = \int_{-h/2}^{h/2} (1, z, z^2) Q_{ij}\, \mathrm{d}z \tag{4}
$$

where h is the plate thickness and Q_{ij} are the plane-stress reduced elastic stiffnesses.

Each of the plies is orthotropic; therefore

$$
\begin{aligned}
A_{ij} &= \sum_{k=1}^{n} Q_{ij}^{(k)}(h_k - h_{k-1}) \\
B_{ij} &= \frac{1}{2}\sum_{k=1}^{n} Q_{ij}^{(k)}(h_k^2 - h_{k-1}^2) \\
D_{ij} &= \frac{1}{3}\sum_{k=1}^{n} Q_{ij}^{(k)}(h_k^3 - h_{k-1}^3)
\end{aligned} \tag{5}
$$

where k denotes a typical ply and n is the total number of plies.

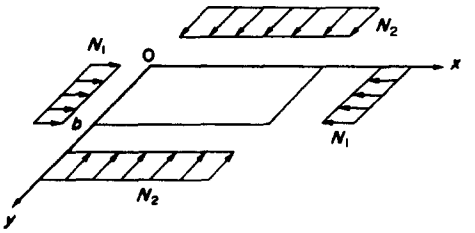

Fig. 1. Rectangular plate subjected to dynamic in-plane loads.

The substitution of eqns (2) and (3) into eqns (1) yields the set of differential equations which can be conveniently represented as[6]

$$[L_{kl}]\begin{Bmatrix} u \\ v \\ w \\ h\psi_y \\ h\psi_x \end{Bmatrix} = \{0\} \tag{6}$$

where $L_{ij} = L_{ji}$ and

$$\begin{aligned}
L_{11} &= A_{11}d_x^2 + A_{66}d_y^2 - C\rho h d_t^2 \\
L_{12} &= (A_{12} + A_{66})d_x d_y \\
L_{13} &= 0 \\
L_{14} &= (B_{16}/h)d_x^2 + (B_{26}/h)d_y^2 \\
L_{15} &= (2B_{16}/h)d_x d_y \\
L_{22} &= A_{66}d_x^2 + A_{22}d_y^2 - C\rho h d_t^2 \\
L_{23} &= 0 \\
L_{24} &= (2B_{26}/h)d_x d_y \\
L_{25} &= L_{14} \\
L_{33} &= -k_5^2 A_{55}d_x^2 - k_4^2 A_{44}d_y^2 + N_1(t)d_x^2 + N_2(t)d_y^2 + \rho h d_t^2 \\
L_{34} &= -(k_4^2 A_{44}/h)d_y \\
L_{35} &= -(k_5^2 A_{55}/h)d_x \\
L_{44} &= (D_{66}/h^2)d_x^2 + (D_{22}/h^2)d_y^2 - (k_4^2 A_{44}/h^2) - (\rho h/12)d_t^2 \\
L_{45} &= (D_{12} + D_{66})h^{-2}d_x d_y \\
L_{55} &= (D_{11}/h^2)d_x^2 + (D_{66}/h^2)d_y^2 - (k_5^2 A_{55}/h^2) - (\rho h/12)d_t^2 \\
d_i &\equiv \partial(\ldots)/\partial i, \qquad i = x, y, t.
\end{aligned} \tag{7}$$

The boundary conditions considered in this paper coincide with those used by Whitney and Leissa[10] and Bert and Chen[6]

$$\begin{aligned}
u(0,y) = u(a,y) &= 0 & N_6(x,0) = N_6(x,b) &= 0 \\
N_6(0,y) = N_6(a,y) &= 0 & v(x,0) = v(x,b) &= 0 \\
w(0,y) = w(a,y) &= 0 & w(x,0) = w(x,b) &= 0 \\
M_1(0,y) = M_1(a,y) &= 0 & M_2(x,0) = M_2(x,b) &= 0 \\
\psi_y(0,y) = \psi_y(a,y) &= 0 & \psi_x(x,0) = \psi_x(x,b) &= 0.
\end{aligned} \tag{8}$$

It is noted that if the shear strains are negligible, these conditions converge to the S3 boundary conditions as defined by Almroth[11] or the SS2 conditions of Hoff[12]. Boundary conditions (8) and governing equations (6) are satisfied if the mode shape of the motion

with m and n half-waves along the x- and y-axes, respectively, is represented by

$$\begin{aligned} u &= U(t)\sin\alpha x\cos\beta y \\ v &= V(t)\cos\alpha x\sin\beta y \\ w &= W(t)\sin\alpha x\sin\beta y \\ h\psi_y &= Y(t)\sin\alpha x\cos\beta y \\ h\psi_x &= X(t)\cos\alpha x\sin\beta y \end{aligned} \tag{9}$$

where

$$\alpha \equiv m\pi/a, \qquad \beta \equiv n\pi/b. \tag{10}$$

The effects of in-plane and rotary inertias on vibrations of antisymmetric angle-ply plates at frequencies near the fundamental frequency are negligible[6]. Since dynamic stability is most important in cases in which the excitation frequencies are of the same order as the fundamental frequency, these inertias are neglected here. Then substitution of eqns (9) into eqns (6) results in the following set of equations:

$$C_{11}U+C_{12}V+C_{14}Y+C_{15}X=0 \tag{11}$$

$$C_{12}U+C_{22}V+C_{24}Y+C_{14}X=0 \tag{12}$$

$$\frac{\rho h^2}{E_T}\ddot{W}+C_{33}W-C_{34}Y-C_{35}X=0 \tag{13}$$

$$C_{14}U+C_{24}V+C_{34}W+C_{44}Y+C_{45}X=0 \tag{14}$$

$$C_{15}U+C_{14}V+C_{35}W+C_{45}Y+C_{55}X=0. \tag{15}$$

where E_T is the Young's modulus in the direction normal to the fibers.

The coefficients C_{ij} are conveniently represented in the non-dimensional form

$$\begin{aligned} C_{11} &= -\bar{A}_{11}\alpha_1^2-\bar{A}_{66}\beta_1^2 \\ C_{12} &= -(\bar{A}_{12}+\bar{A}_{66})\alpha_1\beta_1 \\ C_{14} &= -\bar{B}_{16}\alpha_1^2-\bar{B}_{26}\beta_1^2 \\ C_{15} &= -2\bar{B}_{16}\alpha_1\beta_1 \\ C_{22} &= -\bar{A}_{66}\alpha_1^2-\bar{A}_{22}\beta_1^2 \\ C_{24} &= -2\bar{B}_{26}\alpha_1\beta_1 \\ C_{33} &= k_5^2\bar{A}_{55}\alpha_1^2+k_4^2\bar{A}_{44}\beta_1^2-\bar{N}_1(t)\alpha_1^2-\bar{N}_2(t)\beta_1^2 \\ C_{34} &= -k_4^2\bar{A}_{44}\beta_1 \\ C_{35} &= -k_5^2\bar{A}_{55}\alpha_1 \\ C_{44} &= -\bar{D}_{66}\alpha_1^2-\bar{D}_{22}\beta_1^2-k_4^2\bar{A}_{44} \\ C_{45} &= -(\bar{D}_{12}+\bar{D}_{66})\alpha_1\beta_1 \\ C_{55} &= -\bar{D}_{11}\alpha_1^2-\bar{D}_{66}\beta_1^2-k_5^2\bar{A}_{55}. \end{aligned} \tag{16}$$

Here

$$\alpha_1 \equiv m\pi h/a, \qquad \beta_1 \equiv n\pi\lambda h/a, \qquad \lambda \equiv a/b \tag{17}$$

$$\bar{N}_i(t) = N_i(t)/E_T h; \quad i = 1, 2. \tag{18}$$

The non-dimensional extensional, coupling, and bending stiffnesses, calculated under the assumption that the thickness of each n plies is h/n, can be represented as

$$\begin{aligned} \bar{A}_{ij} &= \sum_{k=1}^{n} \bar{Q}_{ij}^{(k)}/n \\ \bar{B}_{ij} &= (1/2) \sum_{k=1}^{n} \bar{Q}_{ij}^{(k)} f_i(k) \\ \bar{D}_{ij} &= (1/3)\Sigma\bar{Q}_{ij}^{(k)} f_2(k) \end{aligned} \tag{19}$$

where $f_1(k)$ and $f_2(k)$ are given by

$$\begin{aligned} f_1(k) &= (h_k^2 - h_{k-1}^2)/h^2 \\ f_2(k) &= (h_k^3 - h_{k-1}^3)/h^3. \end{aligned} \tag{20}$$

The non-dimensional reduced stiffnesses of the kth ply which is inclined at an angle θ to the x-axis are

$$\begin{aligned} \bar{Q}_{11}^{(k)} &= Q_{11}^* c^4 + 2(Q_{12}^* + 2Q_{66}^*)c^2 s^2 + Q_{22}^* s^4 \\ \bar{Q}_{12}^{(k)} &= (Q_{11}^* + Q_{22}^* - 4Q_{66}^*)s^2 c^2 + Q_{12}^*(s^4 + c^4) \\ \bar{Q}_{22}^{(k)} &= Q_{11}^* s^4 + 2(Q_{12}^* + 2Q_{66}^*)s^2 c^2 + Q_{22}^* c^4 \\ \bar{Q}_{16}^{(k)} &= (Q_{11}^* - Q_{12}^* - 2Q_{66}^*)sc^3 + (Q_{12}^* - Q_{22}^* + 2Q_{66}^*)s^3 c \\ \bar{Q}_{26}^{(k)} &= (Q_{11}^* - Q_{12}^* - 2Q_{66}^*)s^3 c + (Q_{12}^* - Q_{22}^* + 2Q_{66}^*)sc^3 \\ \bar{Q}_{44}^{(k)} &= Q_{44}^* c^2 + Q_{55}^* s^2 \\ \bar{Q}_{55}^{(k)} &= Q_{44}^* s^2 + Q_{55}^* c^2 \\ \bar{Q}_{66}^{(k)} &= (Q_{11}^* + Q_{22}^* - 2Q_{12}^* - 2Q_{66}^*)s^2 c^2 + Q_{66}^*(s^4 + c^4) \end{aligned} \tag{21}$$

where

$$c = \cos\theta; \qquad s = \sin\theta \tag{22}$$

and

$$\begin{aligned} Q_{11}^* &\equiv \frac{E_L/E_T}{1 - \nu_{LT}\nu_{TL}} \\ Q_{12}^* &\equiv \frac{\nu_{LT}}{1 - \nu_{LT}\nu_{TL}} \\ Q_{22}^* &\equiv \frac{1}{1 - \nu_{LT}\nu_{TL}} \\ Q_{44}^* &\equiv G_{TZ}/E_T \\ Q_{55}^* &\equiv G_{LZ}/E_T \\ Q_{66}^* &\equiv G_{LT}/E_T. \end{aligned} \tag{23}$$

The set of eqns (11)–(15) can be reduced to a single equation in W. Indeed, U and V can be expressed in terms of X, Y using eqns (11) and (12)

$$\begin{aligned} U &= S_1 X + S_2 Y \\ V &= S_3 X + S_4 Y \end{aligned} \tag{24}$$

where

$$\begin{aligned} S_1 &= (C_{14}C_{12} - C_{15}C_{22})/S \\ S_2 &= (C_{12}C_{24} - C_{22}C_{14})/S \\ S_3 &= (C_{15}C_{22} - C_{11}C_{14})/S \\ S_4 &= (C_{14}C_{22} - C_{11}C_{24})/S \\ S &= C_{11}C_{22} - C_{12}^2. \end{aligned} \tag{25}$$

After substitution of eqns (24) into eqns (14) and (15), one can express X and Y as

$$X = F_1 W/C_{35}; \qquad Y = F_2 W/C_{34}. \tag{26}$$

Here

$$\begin{aligned} F_1 &\equiv \frac{(C_{35}S_6 - C_{34}S_8)C_{35}}{S_5 S_8 - S_6 S_7} \\ F_2 &\equiv \frac{(C_{34}S_7 - C_{35}S_5)C_{34}}{S_5 S_8 - S_6 S_7} \end{aligned} \tag{27}$$

where

$$\begin{aligned} S_5 &= C_{14}S_1 + C_{24}S_3 + C_{45} \\ S_6 &= C_{14}S_2 + C_{24}S_4 + C_{44} \\ S_7 &= C_{15}S_1 + C_{14}S_3 + C_{55} \\ S_8 &= C_{15}S_2 + C_{14}S_4 + C_{45}. \end{aligned} \tag{28}$$

Now eqns (26) can be substituted into eqn (13) resulting in the linear second-order differential equation for $W(t)$. Representing the non-dimensional pulsating loads by

$$\begin{aligned} \bar{N}_1(t) &= \bar{N}_1^* \cos 2\tau \\ \bar{N}_2(t) &= \bar{N}_2^* \cos 2\tau \end{aligned} \tag{29}$$

where the non-dimensional time parameter is

$$\tau = \omega t \tag{30}$$

one obtains Mathieu's equation

$$W_{,\tau\tau} + (a_0 - 2q \cos 2\tau)W = 0 \tag{31}$$

where

$$\begin{aligned} a_0 &= (1/\bar{\omega}^2)(k_5^2 \bar{A}_{55}\alpha_1^2 + k_4^2 \bar{A}_{44}\beta_1^2 - F_1 - F_2)(a/h)^4 \\ q &= (1/2\bar{\omega}^2)(\bar{N}_1^*\alpha_1^2 + \bar{N}_2^*\beta_1^2)(a/h)^4. \end{aligned} \tag{32}$$

The non-dimensional frequency squared is

$$\bar{\omega}^2 = (\rho a^4/E_T h^2)\omega^2. \tag{33}$$

The boundaries of the instability regions of the solutions of Mathieu's equation are tabulated. It is convenient to use the series representation of these boundaries[13]. For example, the boundaries of the first (principal) instability region are given by

$$a_0 = 1 \mp q - \tfrac{1}{8}q^2 \pm \tfrac{1}{64}q^3 - \cdots \tag{34}$$

if q is small enough so that the series converges. The higher instability regions are not always realized if the plate vibrates with limited amplitudes due to damping.

It is convenient to show the boundaries of the instability regions on the frequency–load plane where the horizontal axis corresponds to the squared non-dimensional frequency of dynamic load $\bar{\omega}^2$ and the vertical axis represents the non-dimensional amplitude of the load N_1^*. Note that $\bar{N}_2^*$ can always be represented as a certain fraction of $\bar{N}_1^*$, so that such representation is possible even if the dynamic loads are applied along both axes.

If the amplitude values $\bar{N}_1^*$, $\bar{N}_2^*$ are small so that non-linear terms in eqn (34) can be neglected, the boundaries of the principal instability region are represented by the following relations:

$$\bar{\omega}^2 = (a/h)^4[(k_5^2\bar{A}_{55}\alpha_1^2 + k_4^2\bar{A}_{44}\beta_1^2 - F_1 - F_2) \mp (1/2)(\bar{N}_1^*\alpha_1^2 + \bar{N}_2^*\beta_1^2)]. \tag{35}$$

3. RESULTS AND DISCUSSION

Two plates were considered: a two-layer plate ($\theta = -45°/45°$) and a four-layer plate ($\theta = 45°/-45°/45°/-45°$). The material properties were taken as in Refs [3, 6], i.e.

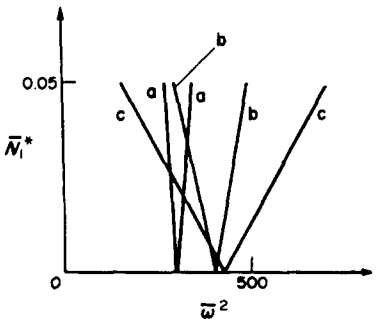

Fig. 2. Effect of relative thickness on the principal instability region for a two-layer (−45°, 45°) square plate; $\bar{N}_2^* = 0$, $m = n = 1$, $k_4^2 = k_5^2 = 5/6$; cases a–c are for $h/a = 0.10$, 0.05, 0.03, respectively.

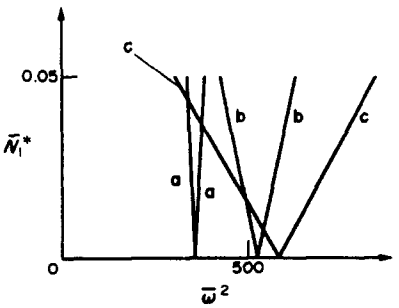

Fig. 3. Effect of relative thickness on the principal instability region for a four-layer (45°, −45°, 45°, −45°) square plate; $\bar{N}_2^* = 0$, $m = n = 1$, $k_4^2 = k_5^2 = 5/6$; cases a–c as in Fig. 2.

$$E_L/E_T = 40, \quad G_{LT}/E_T = G_{LZ}/E_T = 0.6, \quad G_{TZ}/E_T = 0.5, \quad \nu_{LT} = 0.25, \quad k_4^2 = k_5^2 = 5/6.$$

The effect of the relative thickness h/a on the principal instability regions of two- and four-layer square plates is shown in Figs 2 and 3. It appears that the instability regions of thicker plates are narrow. These regions are also shifted to the smaller non-dimensional excitation frequencies. However, if we calculate the dimensional frequencies using eqn (33), the instability regions of thicker plates correspond to larger frequencies. This reflects the fact that the thicker plates are stiffer. The increase of the aspect ratio is shown to shift the instability regions to the larger excitation frequencies as shown in Figs 4 and 5.

The effect of the magnitude of the shear correction coefficients which were otherwise supposed to be equal to 5/6 is shown in Figs 6 and 7. The larger shear correction coefficients result in the shift of the principal instability region to the smaller frequencies. Finally, the effect of the number of layers on the instability region of a square plate is shown in Fig. 8. The increase of the number of layers shifts the instability region to larger frequencies; in this particular case, the width of the principal instability region was not essentially influenced by the number of layers.

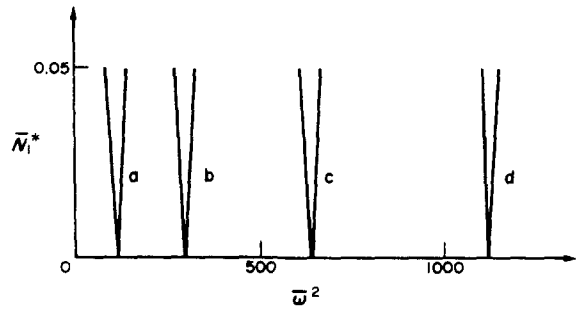

Fig. 4. Effect of aspect ratio on the principal instability region for a two-layer (−45°, 45°) plate; $\bar{N}_2^* = 0$, $h/a = 0.1$, $m = n = 1$, $k_4^2 = k_5^2 = 5/6$; cases a–d are for $\lambda = 0.5, 1.0, 1.5, 2.0$, respectively.

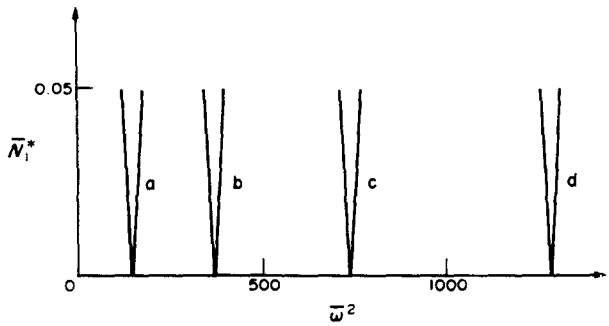

Fig. 5. Effect of aspect ratio on the principal instability region for a four-layer (45°, −45°, 45°, −45°) plate; $\bar{N}_2^* = 0$, $h/a = 0.1$, $m = n = 1$, $k_4^2 = k_5^2 = 5/6$; cases a–d as in Fig. 4.

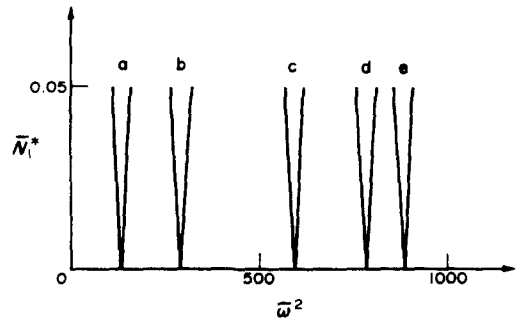

Fig. 6. Effect of the shear correction coefficients on the principal instability region for a two-layer (−45°, 45°) square plate; $\bar{N}_2^* = 0$, $h/a = 0.1$, $m = n = 1$; cases a–e correspond to values of $k_4^2 = k_5^2$ of 1.0, 0.833, 0.50, 0.25, and 0, respectively.

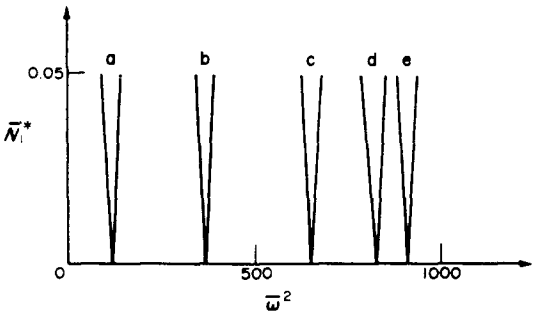

Fig. 7. Effect of the shear correction coefficients on the principal instability region for a four-layer (45°, −45°, 45°, −45°) square plate; $\bar{N}_2^* = 0$, $h/a = 0.1$, $m = n = 1$; cases a–e as in Fig. 6.

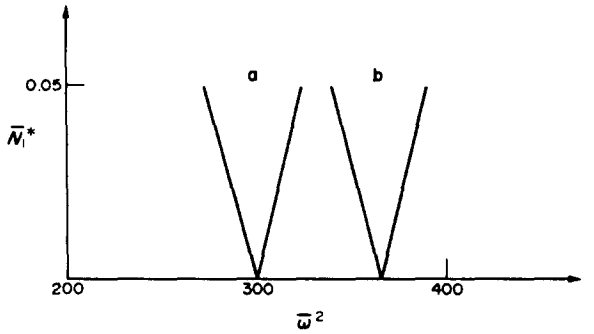

Fig. 8. Effect of number of layers on the principal instability region of a square plate; $\bar{N}_2^* = 0$, $h/a = 0.1$, $m = n = 1$, $k_4^2 = k_5^2 = 5/6$; cases a and b correspond to two and four layers, respectively.

In conclusion, the effect of shear deformation on dynamic stability of antisymmetrically laminated angle-ply plates is significant. This is consistent with results obtained in previous work considering vibration, buckling, and static deflection of such plates.

REFERENCES

1. C. W. Bert, Analysis of plates. In *Structural Design and Analysis*, Part I (Edited by C. C. Chamis), Chap. 4, p. 149. Academic Press, New York (1974).
2. C. W. Bert, A critical evaluation of new plate theories applied to laminated composites. *Composite Struct.* **2**, 329 (1984).
3. P. C. Yang, C. H. Norris and Y. Stavsky, Elastic wave propagation in heterogeneous plates. *Int. J. Solids Structures* **2**, 665 (1966).
4. J. M. Whitney and N. J. Pagano, Shear deformation in heterogeneous anisotropic plates. *J. Appl. Mech.* **37**, 1031 (1970).
5. A. K. Noor, Stability of multilayered composite plates. *Fibre Sci. Technol.* **8**, 81 (1975).
6. C. W. Bert and T. L. C. Chen, Effect of shear deformation on vibration of antisymmetric angle-ply laminated rectangular plates. *Int. J. Solids Structures* **14**, 465 (1978).
7. S. Srinivas and A. K. Rao, Bending, vibration and buckling of simply supported thick orthotropic rectangular plates and laminates. *Int. J. Solid Structures* **6**, 1463 (1970).
8. C. T. Sun and J. M. Whitney, Theories for the dynamic response of laminated plates. *AIAA J.* **11**, 178 (1973).
9. V. Birman, Dynamic stability of unsymmetrically laminated rectangular plates. *Mech. Res. Commun.* **12**, 81 (1985).
10. J. M. Whitney and A. W. Leissa, Analysis of heterogeneous anisotropic plates. *J. Appl. Mech.* **36**, 261 (1969).
11. B. O. Almroth, Influence of edge conditions on the stability of axially compressed cylindrical shells. *AIAA J.* **4**, 134 (1966).
12. N. J. Hoff, The perplexing behavior of thin cylindrical shells in axial compression, *Israel J. Technol.* **4**, 1 (1966).
13. N. W. McLachlan, *Theory and Application of Mathieu Functions*. Dover, New York (1964).